Inorg. Chem. **2007**, *46*, 6078–6082

Liquid Crystalline Derivatives of Bis(tricarbollide)Fe(II)

Adam Januszko,[†] Piotr Kaszynski,*[,†] and Bohumír Grüner[‡]

Organic Materials Research Group, Department of Chemistry, Vanderbilt University, Box 1822 Station B, Nashville, Tennessee 37235, and Institute of Inorganic Chemistry, Academy of Sciences of the Czech Republic, 25068 Rez, The Czech Republic

Received March 29, 2007

A series of Schiff bases **2[*n*]** with $n = 4$, 6, 8, 10, 12, and 18 was prepared by the condensation of 9,9′-diaminobis-(tricarbollide)Fe(II) (**1b**) with appropriate 4-alkoxybenzaldehydes (**3[*n*]**). Thermal analysis showed that they form nematic and smectic phases with clearing temperatures above 200 °C. Comparative studies of series **2[*n*]** and its organic analogs demonstrated that the effectiveness of bis(tricarbollide)Fe(II) in supporting liquid crystalline phases is between that of benzene and biphenyl for $n \leq 18$ and lower than that of benzene for $n = \infty$. The photophysical properties were investigated for the butoxy derivative **2[4]** and modeled using ZINDO calculations.

Introduction

A vast majority of metallomesogens (liquid crystalline organometallic compounds) are *sigma* complexes in which the metal is coordinated to the lone pairs of heteroatoms in, e.g., β-diketonates, dithiocarboxylates, or phthalocyanines.[1] There are only a handful of mesogenic metal−ligand π complexes, and all of them are derived from two metallocenes (ferrocene[2] and ruthenocene[3]), butadieneiron(II) tricarbonyl,[4] and benzenechromium tricarbonyl.[5] In these metallomesogens the long molecular axis is parallel to the coordinated π system, and they can be classified as type I (Figure 1). In type II metallomesogens the long molecular axis is perpendicular to the π system of the ligand, and, to our knowledge, such compounds have not been studied experimentally to date. Both of these topologies are of interest for the development of multifunctional liquid crystalline materials exhibiting, e.g., magnetic anisotropy.

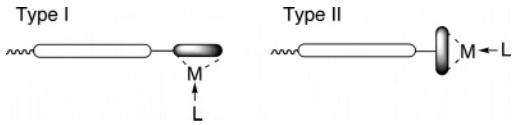

Figure 1. Two possible topologies for mesogenic metal π-complexes. The gray element represents the plane of the π system that is coordinated to the metal, and the white element is a mesogenic substituent. Ligand L may also carry a mesogenic fragment.

Type II metallomesogens could, in principle, be provided by metal complexes of some *nido*-carboranes,[6] which upon substitution in the antipodal positions give rise to highly anisometric molecules. Particularly attractive in this context are *nido*-carborane anions $C_2B_9H_{11}^{2-}$ (**A** and **B**) and $C_2B_4H_6^{2-}$ (**C**) in Figure 2, which are isolobal[7] with the cyclopentadienyl anion, $C_5H_5^-$, and their numerous complexes with transition metals have been prepared and extensively reviewed.[8,9] With

* To whom correspondence should be addressed. Phone: 615-322-3458. Fax: 615-343-1234. E-mail: piotr.kaszynski@vanderbilt.edu.
[†] Vanderbilt University.
[‡] Academy of Sciences of the Czech Republic.

(1) Donnio, B.; Guillon, D.; Deschenaux, R.; Bruce, D. W. Metallomesogens. In *Comprehensive Coordination Chemistry II*; McCleverty, J. A., Meyer, T. J., Eds.; 2004; Vol. 7, pp 357−627. *Metallomesogens: Synthesis, Properties and Applications*; Serrano, L. J., Ed.; Wiley-VCH: New York, 1996.
(2) Chuard, T.; Deschenaux, R. *Chimia* **2003**, *57*, 597−600. *Ferrocenes: homogeneous catalysis, organic synthesis, materials science;* Togni A., Hayashi, T., Eds.; VCH Publishers: New York, 1995.
(3) Deschenaux, R.; Santiago, J. *J. Mater. Chem.* **1993**, *3*, 219−220.
(4) Ziminski, L.; Malthete, J. *J. Chem. Soc., Chem. Commun.* **1990**, 1495−1496. Huang, D.; Yang J.; Wan, W.; Ding, F.; Zhang, L.; Liu, Y.; Xiang, S. *Mol. Cryst. Liq. Cryst*. **1996**, *281*, 43−49.
(5) Campillos, E.; Deschenaux, R.; Levelut, A.-M.; Ziessel, R. *J. Chem. Soc., Dalton Trans*. **1996**, 2533−2536. Yang, J.; Huang, D.; Ding, F.; Zhao, K.; Guan, W.; Zhang, L. *Mol. Cryst. Liq. Cryst*. **1996**, *281*, 51−56.
(6) Grimes, R. N. Transition Metal Metallacarboranes. In *Comprehensive Organometallic Chemistry II*; Abel, E. W., Stone, F. G. A., Wilkinson, G., Housecroft, C. E., Eds.; Pergamon: Exeter, U.K., 1995; Vol. 1, pp 373−430. Grimes, R. N. Metallacarboranes and Metallaboranes. In *Comprehensive Organometallic Chemistry;* Wilkinson, G., Stone, F. G. A., Abel, E. W., Eds.; Pergamon Press: New York, 1982; Vol. 1, pp 459−542. Dunks, G. B.; Hawthorne, M. F. In *Boron Hydride Chemistry*; Muetterties, E. L., Ed.; Academic Press: New York, 1975; pp 383−430.
(7) Hanusa, T. P. *Polyhedron* **1982**, *1*, 663−665.
(8) For example: Sivaev, I. B.; Bregadze, V. I. *J. Organomet. Chem.* **2000**, *614−615*, 27−36. Sivaev, I. B.; Bregadze, V. I. *Collect. Czech. Chem. Commun*. **1999**, *64*, 783−805. Saxena, A. K.; Hosmane, N. S. *Chem. Rev.* **1993**, *93*, 1081−1124.
(9) Grimes, R. N. *Pure Appl. Chem.* **2003**, *75*, 1211−1218. Grimes, R. N. *Collect. Czech. Chem. Commun*. **2002**, *67*, 728−750. Grimes, R. N. *Coord. Chem. Rev*. **2000**, *200*, 773−811.

10.1021/ic7005937 CCC: $37.00
Published on Web 06/28/2007

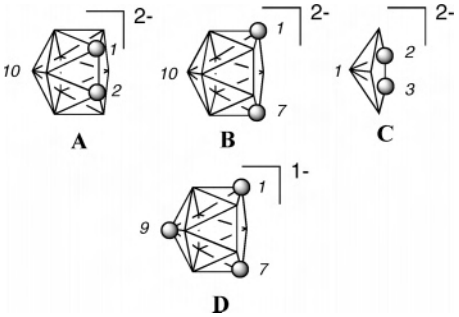

Figure 2. Selected *nido*-carborane anions suitable for metallomesogens of type II. Each vertex represents a BH fragment, and the sphere is a CH group.

Scheme 1

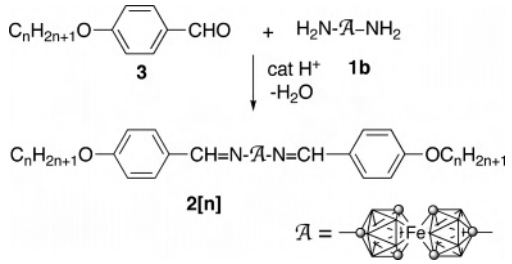

a few notable exceptions,[10,11] most of these complexes are negatively charged, and, more importantly, the appropriate 10,10′-difunctionalized carbollides are not available. These factors were serious obstacles in the investigation of liquid crystalline derivatives of these complexes. Recently, an electrically neutral complex of 1,7,9-tricarbaundecaborate (**D**) and iron(II) (**1a**) was prepared, and two amino groups were introduced in the antipodal positions 9 and 9′.[12] The availability of this functionalized bis(tricarbollide)Fe(II) **1b** provides the first opportunity to prepare and investigate metallomesogens of type II.

Here we demonstrate the first liquid crystalline derivative of a boron cluster−metal complex. Thus, we investigate mesogenic properties of a homologous series **2[*n*]** derived from diamine **1b** and assess the effectiveness of

bis(tricarbollide)Fe(II) (**1a**) as a structural element of liquid crystals. We also probe the extent of electronic interactions between the π substituents and the tricarbollide by means of electronic absorption spectroscopy augmented by ZINDO calculations.

Results and Discussion

Synthesis. Schiff bases **2[*n*]** were prepared by acid-catalyzed condensation of diamine **1b**[12] with appropriate aldehydes **3[*n*]** (Scheme 1). Products were purified by repeated crystallization.

Table 1. Transition Temperatures (°C) and Enthalpies (kJ/mol) for **2[*n*]**[a]

	phase transitions					
2[4]	Cr_1 154 (8.6)	Cr_2 162 (7.2)	Cr_3 211 (37.1)	SmA 213 (0.1)[d]	N > 370[b,c]	
2[6]	Cr_1 137 (25.5)	Cr_2 190 (0.8)	Cr_3 204 (32.3)	N ∼ 365[b,c]	I	
2[8]	Cr_1 91 (2.9)	Cr_2 166 (38.4)	N 317[c] (2.5)	I		
2[10]	Cr 153 (34.2)	(SmA 133)[e,f]	N 286[c] (3.0)	I		
2[12]	Cr_1 119 (12.0)	Cr_2 129 (21.5)	(SmC 110 (∼0.1)[d]	SmA 118)[e] (0.1)[d]	N 258 (3.8)	I
2[18]	Cr_1 97 (20.6)	Cr_2 111 (100.0)	SmC 191	SmA 194 (2.3)[g]	N 209 (2.5)	I

[a] Cr - crystal, Sm - smectic, N - nematic, I - isotropic, observed in the heating mode. [b] Decomposition. [c] Scan rate 25 °C/ min. [d] Enthalpy obtained on cooling. [e] Monotropic transition. [f] Microscopic observation. [g] Combined enthalpy for SmC-SmA and SmA-N transitions.

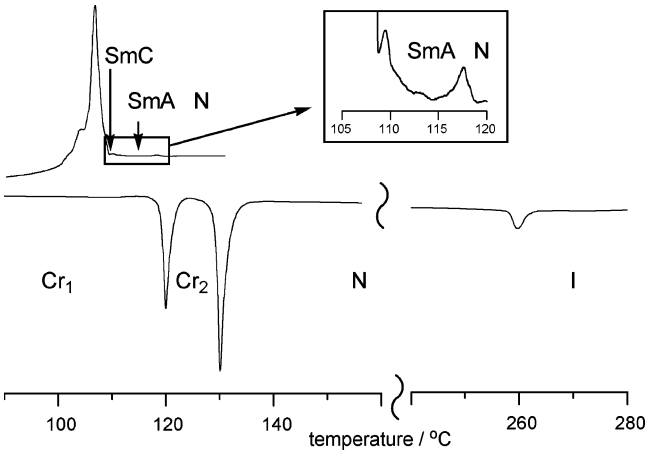

Figure 3. A DSC trace for **2[12]** obtained on heating (lower trace) and on cooling (upper trace) at a scanning rate of 5 °C min^{-1}. The expanded region of 105−120 °C is shown in the inset.

Mesogenic Properties. Transition temperatures and enthalpies of **2[*n*]** were determined by differential scanning calorimetry (DSC), and the results are shown in Table 1.

All compounds show enantiotropic nematic phases with clearing temperatures of over 200 °C. The clearing temperature for the butoxy derivative **2[4]** was not observed, and for the hexyloxy derivative **2[6]** the T_{NI} is uncertain due to the sample's volatility and instability above 350 °C. Based on microscopic observations, the T_{NI} for **2[6]** was estimated to be in the region of 365−370 °C. Clearing temperatures for the higher members of the homologous series were detected by DSC, as shown for **2[12]** in Figure 3, and they monotonically decrease to 209 °C observed for **2[18]**.

Smectic phases are significantly less stable than nematic phases in series **2[*n*]** which is consistent with our findings for carborane-containing mesogens.[13,14] The butoxy derivative **2[4]** exhibits a narrow range enantiotropic SmA phase with the SmA-N transition at 213 °C. The texture of the smectic phase grown from the nematic phase was focal-conic, which is typical for a SmA phase and is shown in Figure 4.

No smectic behavior was detected by optical microscopy in the hexyloxy **2[6]** nor in octyloxy **2[8]** even in samples

(10) Warren, L. F., Jr.; Hawthorne, M. F. *J. Am. Chem. Soc.* **1967**, *89*, 470−471.
(11) Wang, X.; Sabat, M.; Grimes, R. N. *J. Am. Chem. Soc.* **1995**, *117*, 12218−12226.
(12) Grüner, B.; Bačkovský, J.; Sillanpää, R.; Kivekäs, R.; Císačová, I.; Teixidor, F.; Viñas, C.; Štíbr, B. *Eur. J. Inorg. Chem.* **2004**, 1402−1410.

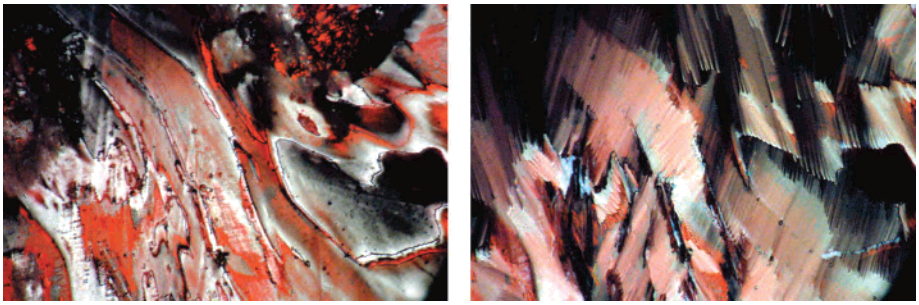

Figure 4. Textures observed in polarized light for **2[4]:** (a) N phase at ~220 °C and (b) SmA at ~210 °C. Magnification 60×.

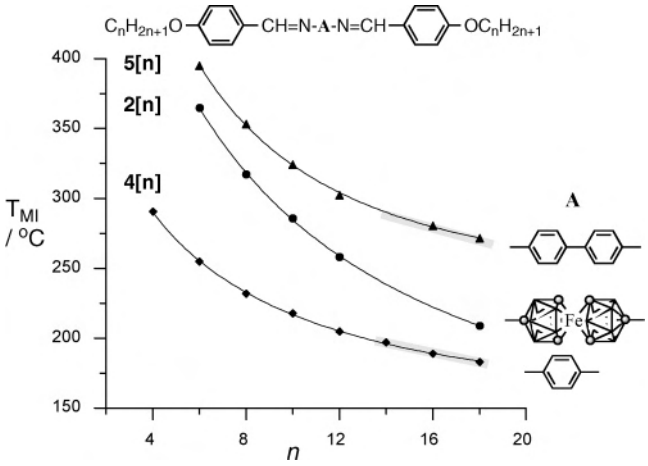

Figure 5. Clearing temperatures T_{NI} and T_{SI} (outlined in gray) for a series of mesogens as a function of the chain length *n*.

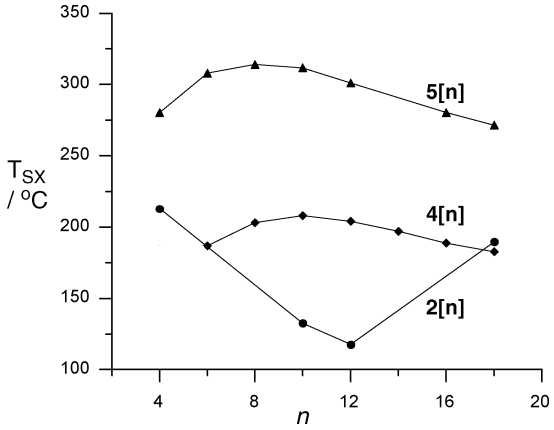

Figure 6. Sm−N or Sm−I transition temperatures, T_{SX}, in the homologous series. Lines are included as a guide for the eye.

supercooled by nearly 60 °C. Monotropic smectic phases were observed in **2[10]** and **2[12]** (Figure 3), and broad-range enantiotropic smectic behavior was found in **2[18]**. The decyloxy derivative **2[10]** exhibits a SmA phase 20 °C below the melting temperature and crystallizes just below the Sm−N transition. Compound **2[12]** shows a schlieren texture SmC phase below the SmA, and **2[18]** exhibits both SmA and SmC as enantiotropic phases.

To gain a better understanding of the effectiveness of the bis(tricarbollide)Fe(II) in stabilization of liquid crystalline phases, the mesogenic behavior of series **2[*n*]** was compared to that of structurally analogous benzene[15] and biphenyl[16] derivatives, **4[*n*]** and **5[*n*]**.[17] A comparison in Figure 5 shows that the clearing temperatures for the tricarbollides **2[*n*]** fall in between those for the benzene and biphenyl series. In all three series there is an early onset of smectic polymorphism (Figure 6). In the aromatic series, the Sm−N transition temperatures, T_{SN}, exhibit a maximum for $n = 10$ in **4[*n*]** and for $n = 8$ in **5[*n*]**. Also both series display a rich smectic and soft crystal polymorphism, which completely replaces the nematic phase for $n = 14$. In contrast, the T_{SN} values for tricabollides **2[*n*]** appear to have a minimum, presumably for $n = 12$, the smectic polymorphism is limited to SmA and SmC, and even **2[18]** still exhibits a 16 °C wide nematic phase.

Numerical analysis of the clearing temperatures revealed an exponential decay of the T_{MI} values with increasing chain length in all three series (Figure 5). The data were fitted to a three-parameter function[18] (eq 1) previously used in a similar analysis of other homologous series.[14] The full forms of the three-parameter fitting functions for all three series are shown in the Supporting Information.

$$T_{MI} = a + \exp(b \times \sqrt{n} + c) \qquad (1)$$

Results for series **2[*n*]** and **4[*n*]** showed a high correlation factor R^2 of >0.999, which is expected for compounds of high purity and internally consistent measurements. In contrast, the R^2 factor was lower for the series of biphenyl derivatives **5[*n*]**. Inspection of the fit revealed that the high temperature point for **5[6]** appeared low, which might be due to the generally lower reliability of temperature measurements above 350 °C. An excellent fit was obtained when

(13) Douglass, A. G.; Czuprynski, K.; Mierzwa, M.; Kaszynski, P. *Chem. Mater*. **1998**, *10*, 2399−2402. Czuprynski, K.; Douglass, A. G.; Kaszynski, P.; Drzewinski, W. *Liq. Cryst.* **1999**, *26*, 261−269. Czuprynski, K.; Kaszynski, P. *Liq. Cryst*. **1999**, *26*, 775−778. Ringstrand, B.; Vroman, J.; Jensen, D.; Januszko, A.; Kaszynski, P.; Dziaduszek, J.; Drzewinski, W. *Liq. Cryst*. **2004**, *32*, 1061−1070.
(14) Nagamine, T.; Januszko, A.; Ohta, K.; Kaszynski, P.; Endo, Y. *Liq. Cryst*. **2005**, *32*, 985−995. Nagamine, T.; Januszko, A.; Ohta, K.; Kaszynski, P.; Endo, Y. *J. Mater. Chem*. **2006**, *16*, 3836−3843.
(15) Arora, S. L.; Fergason, J. L.; Taylor, T. R. *J. Org. Chem.* **1970**, *35*, 4055−4058. Arora, S. L.; Taylor, T. R.; Fergason, J. L.; Saupe, A. *J. Am. Chem. Soc*. **1969**, *91*, 3671−3673.
(16) Gray, G. W.; Hartley, J. B.; Ibbotson, A.; Jones, B. *J. Chem. Soc.* **1955**, 4359−4368.
(17) For details see the Supporting Information.
(18) Other empirical functions used for the description of trends in T_{MI} within homologous series are less satisfactory and provide less rigorous tests for self-consistency of the data. For example Averyanov, E. M. *Russ. J. Phys. Chem*. **2003**, *77*, 1237−1246.

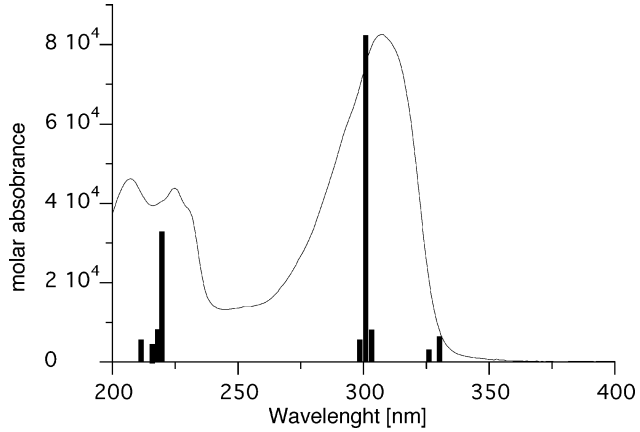

Figure 7. Electronic absorption spectrum for **2[4]** recorded in cyclohexane. Vertical bars represent the calculated transition energies for **2[1]** constrained at the C_i symmetry. The size of the bars corresponds to the oscillator strength. Only transition with $f > 0.1$ are shown.

the reported clearing temperature for **5[6]** (384 °C) was assumed to be 11 °C higher.

An analysis of the fitting functions shows that the biphenyl and benzene series, **5[*n*]** and **4[*n*]**, have high limiting values a [$\lim_{n\to\infty} T_{MI}(n) = a$] of 237 ± 5 °C and 149 ± 3 °C, respectively. In contrast, the tricarbollides **2[*n*]** exhibit a steeper descent in the T_{NI} in the series (Figure 5), and consequently the $T_{MI}(\infty)$ is the lowest among the three series (113 ± 12 °C). A similar rapid destabilization of the nematic phases with the increasing *n* was observed for the carborane homologous series.[14] It was ascribed to higher conformational mobility of the molecules resulting from the nearly flat 5-fold rotational potential of the substituent−carborane bond, which unfavorably affects the dynamic aspect ratio of the molecules and consequently decreases the mesophase stability.

The fitting equations permit an estimate of the missing clearing temperatures for derivatives in each homologous series. Thus, for **2[4]** the estimated T_{NI} is 434 °C, and for the biphenyl analog **5[4]** it is 468 °C, well beyond the thermal stability of these derivatives. The shortest derivative of the benzene series, **4[2]**, has an estimated clearing temperature of 353 °C, which is consistent with the reported[16] value >330 °C.

Absorption Spectroscopy. To assess the extent of electronic interactions between the bis(tricarbollide)Fe(II) and the π substituents in series **2[*n*]**, we recorded the UV spectrum for **2[4]** and analyzed it with the aid of quantum-mechanical methods. For the latter, we chose ZINDO,[19] a semiempirical method that is well suited for studying transition-metal derivatives, which gives reasonably good agreement between calculated and experimental electronic transitions and is very efficient for large molecules such **2-[*n*]**.

The spectrum shown in Figure 7 consists of a group of medium intensity absorption bands below 240 nm, a dominant absorption band with a λ_{max} at 307 nm ($\epsilon = 8.1 \times 10^4$), and a broad low intensity absorbance ($\epsilon = 2.5 \times 10^2$) in the

(19) Zerner, M. *Reviews in Computational Chemistry*; Lipkowitz, K. B., Boyd, D. B., Eds.; VCH: New York, 1991; Vol. 2, p 313.

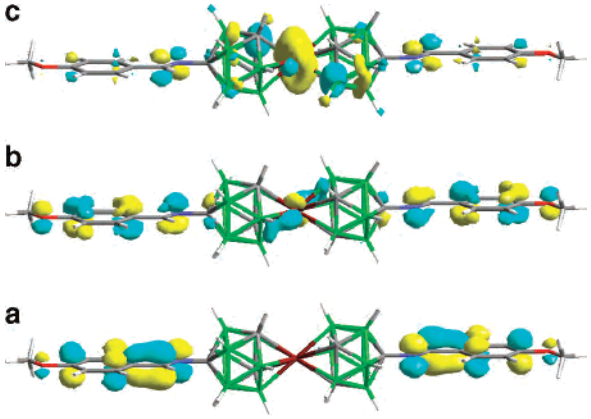

Figure 8. HOMO−1 (a), HOMO (b), and LUMO (c) contours calculated (INDO-2//INDO-2) for **2[1]** at the C_i geometry.

range of 430−580 nm with a maximum at 494 nm. ZINDO calculations performed for **2[1]**, which was constrained at the C_i point group symmetry, reproduced the experimental spectral features of **2[4]** well. Analysis of the computational results revealed that the most intense absorption calculated at 301 nm ($f = 1.96$) has a longitudinal transition moment and originates from a combination of the HOMO-1 − LUMO, HOMO-1 − LUMO+1, and HOMO − LUMO+2 excitations. Three of the four orbitals involved in this transition are shown in Figure 8. The occupied orbitals are localized either exclusively on the π-aromatic fragment $-C_6H_4-CH=N$ (HOMO-1) or with a small contribution from the Fe atom (HOMO). The LUMO and LUMO+1 are mainly localized on the Fe center and to a smaller extent on the $-CH=N-$ π system.

The broad absorption band around 500 nm involves mainly the d−d transitions and is responsible for the orange-red color of the material. The INDO/2 results show four such transitions calculated at 480 nm, 490, 618, and 768 nm.

For comparison, the absorption spectrum was also calculated for the parent bis(tricarbollide)iron(II) (**1a**) constrained at the C_{2h} symmetry. Analysis revealed that the absorption bands in the visible region are practically unchanged by the substitution with the π-aromatic groups in **2[1]**. The most intense absorption band in **1a** is calculated at 284 nm ($f =$ 0.39) and involves the excitation from the HOMO-1, localized on the tricarbollide subunit, to LUMO+1, which is almost entirely localized on the iron center. This transition appears to be replaced by the substantially more intense and lower energy π-to-metal transition in **2[1]**. A similar change in the UV spectrum was observed for *p*-carborane upon substitution with π-aromatic groups.[20]

Summary and Conclusions

Results show that bis(tricarbollide)Fe(II) **1a** is an effective structural element for liquid crystals and has qualitatively similar impact as *p*-carborane on bulk and molecular properties of the mesogens. Thus, like the carborane analogs, the series **2[*n*]** shows a relatively steep decrease of the T_{NI} with

(20) Kaszynski, P.; Kulikiewicz, K. K.; Januszko, A.; Douglass, A. G.; Tilford, R. W.; Pakhomov, S.; Patel, M. K.; Radziszewski, G. J.; Young, V. G., Jr. Unpublished results.

increasing *n*, a preference for the nematic phase, and a strong absorption band due to π substituent−cage excitation. The ability of bis(tricarbollide)Fe(II) to support the mesogenic phase appears to be greater than that of *p*-carborane, and it is between that for biphenyl and benzene for $n \leq 18$.

The presented results indicate new opportunities in the design, synthesis, and characterization of metallomesogens of type II with custom-tailored properties. This can be achieved not only by using other derivatives of **1a** but also by judicious choice of the transition metal and also by the use of other properly substituted *nido*-carboranes.

Computational Details

Geometry optimization for **2[1]** constrained at the C_i point group symmetry was carried out with the INDO/2 algorithm and default convergence limits. Electronic spectra were calculated using the same algorithm. The INDO/2 algorithm is part of the ZINDO 3.5 suite of programs implemented in the Cerius2.

Experimental Section

Optical microscopy and phase identification were performed using a PZO "Biolar" polarized microscope equipped with a HCS402 Instec hot stage. Thermal analysis was performed using a TA Instruments 2920 DSC. Transition temperatures (onset) and enthalpies were obtained using small samples (1−2 mg) and a heating rate of 5 or 25 °C·min^{-1} under the flow of nitrogen gas. For DSC and microscopic analyses, each compound was rigorously purified by dissolving in CH_2Cl_2, filtering to remove particles, evaporating, and multiple recrystallization from the indicated solvent until a constant transition temperature was obtained. The resulting crystals were dried in vacuum for an hour at ambient temperature. For such purified sample, the clearing transition was typically less than 0.4 °C wide.

Preparation of Schiff Bases 2[*n*]. General Procedure. A solution of [*closo*-9,9′-$(NH_2)_2$-*commo*-2,2′-Fe(II)-1,7,9-$(C_3B_8H_{10})_2$][12] (**1b**, 30 mg, 0.085 mmol), 4-alkoxybenzaldehyde (**3[*n*]**, 0.20 mmol), and a catalytic amount of TsOH in absolute EtOH (5 mL) was refluxed for 3 h. The solvent was evaporated, and the solid residue was washed with hexane. Analytical samples were obtained by repeated recrystallization. Analytical data (^{1}H NMR, UV, and El. Anal.) for all compounds are listed in the Supporting Information.

4-Alkoxybenzaldehydes **3[*n*]** were prepared according to a modified general literature procedure,[21] and the details are provided in the Supporting Information.

Acknowledgment. This project was supported in part by the NSF (DMR-0111657 and DMR-0606317).

Supporting Information Available: Listings of analytical data for **2[*n*]** and **3[*n*]**, details for numerical analysis of clearing temperatures, and archive for ZINDO computational results. This material is available free of charge via the Internet at http://pubs.acs.org.

IC7005937

(21) Lin, Y.-R.; Hong, Y.-L. V.; Hong, J. L. *Mol. Cryst. Liq. Cryst.* **1994**, *241*, 69−76.